Available online at www.sciencedirect.com
ScienceDirect
Journal of Molecular Catalysis A: Chemical 278 (2007) 209–214
JOURNAL OF MOLECULAR CATALYSIS A: CHEMICAL
www.elsevier.com/locate/molcata

Surface acidic and redox properties of V-Zr-O catalysts for the selective oxidation of toluene to benzaldehyde

Jiazhen Ge [a], Mingwei Xue [a], Qing Sun [a,b], Aline Auroux [b,*], Jianyi Shen [a,*]

[a] *Laboratory of Mesoscopic Chemistry, School of Chemistry and Chemical Engineering, Nanjing University, Nanjing 210093, China*
[b] *Institut de Recherches sur la Catalyse et l'Environnement de Lyon, UMR 5256, CNRS-Université Lyon 1, 2 Avenue Albert Einstein, 69626 Villeurbanne Cedex, France*

Received 16 July 2007; received in revised form 28 August 2007; accepted 1 September 2007
Available online 7 September 2007

Abstract

A series of V-Zr-O (V_2O_5-ZrO_2) complex oxides were prepared by the sol–gel method. The phases of the samples as detected by the X-ray diffraction depended on the content of V_2O_5 in the complex oxides. ZrV_2O_7 was found to be the main phase in the 50% V_2O_5-ZrO_2. The results of temperature programmed reduction showed that the complex oxides V-Zr-O were easier reduced than the single oxides ZrO_2 and V_2O_5, indicating the increased redox ability of the complex oxides. On the other hand, the complex oxides with surface ZrV_2O_7 exhibited the significantly lower surface acidity and relatively stronger redox ability, and thus, the better reactivity for the selective oxidation of toluene to benzaldehyde and benzoic acid.

Keywords: V-Zr-O complex oxides; Surface acidic and redox properties; Isopropanol probe reactions; Selective oxidation of toluene; Benzaldehyde; Benzoic acid

1. Introduction

Caprolactam is a raw material for the synthesis of nylon 66, an important engineering plastic. In the SNIA-Viscosa process [1–3], toluene is a starting material for the synthesis of caprolactam. The first step of the process is the oxidation of toluene to benzoic acid in liquid phase through the free radical mechanism. Such free radical reaction converts toluene mainly into benzoic acid. Only trace of benzaldehyde is formed during the process. However, benzaldehyde is more costly than benzoic acid since it is an important raw material for the synthesis of many other valuable chemicals such as flavors, medicines and pesticides [4]. Thus, the catalytic oxidation of toluene to benzaldehyde in gas phase has received considerable attention [5–19]. For example, Ce-Mo-O and Fe-Mo-O have been studied for the selective oxidation of toluene to benzaldehyde [5–7]. Vanadium based catalysts such as K-V/TiO_2 [8], V-Sb-Ti-O [9], V-SiO_2 [10], V-Ag-O [11] and V-Ag-Ni-O [12] were also studied and usually exhibited better catalytic behavior than molybdenum based ones for the oxidation of toluene to benzaldehyde. However, there is no commercial plant available currently for the production of benzaldehyde from the oxidation of toluene by air in gas phase due to the low activity and/or selectivity.

V_2O_5 supported on ZrO_2 for the selective oxidation of hydrocarbons have been widely studied during the past decades [20–25]. Normally, the loading of V_2O_5 was lower than 25% and the investigations were focused on the effect of loading of V_2O_5 on the catalytic behavior and few reports were found in the literature about the catalytic behavior of the complex V-Zr-O (V_2O_5-ZrO_2) oxides.

In this work, we studied the V-Zr-O catalysts mainly in terms of their surface acidic and redox properties which were attempted to be correlated with the catalytic behavior of these catalysts for the selective oxidation of toluene to benzaldehyde and benzoic acid. Specifically, the surface acidity was characterized by employing the microcalorimetric adsorption of ammonia, while the redox property was revealed by the traditional technique of temperature programmed reduction (TPR). Meanwhile, the surface acidity and redox property as well as their relative importance were probed by the reaction of isopropanol over the catalysts with the presence of O_2.

* Corresponding authors. Tel.: +86 25 83594305; fax: +86 25 83594305.
E-mail address: jyshen@nju.edu.cn (J. Shen).

1381-1169/$ – see front matter © 2007 Elsevier B.V. All rights reserved.
doi:10.1016/j.molcata.2007.09.005

2. Experimental

2.1. Preparation of catalysts

A series of catalysts were prepared by the sol–gel method. According to the desired proportion of V and Zr, NH_4VO_3 and $Zr(NO_3)_4{\cdot}5H_2O$ were dissolved in water, respectively, with some citric acid (the molar ratio of V/citric acid or Zr/citric acid was kept at 1/2). The aqueous solution of NH_4VO_3 was then added with constant stirring to the aqueous solution of $Zr(NO_3)_4$. The pH of the mixture was controlled at 2.0 by the addition of HNO_3. Some polyacrylic acid was also added in order to enhance the dispersion of metal cations and the formation of gel. After stirred for 1 h, the sol was evaporated in a water bath at 353 K until the gel was formed. After being dried at 393 K for 12 h, the sample was calcined in a muffle furnace at 723 K for 4 h. The sample was then pelletized, crushed and sieved to 20–40 meshes for the catalytic tests.

2.2. Characterization of catalysts

The surface areas were measured by N_2 adsorption at the temperature of liquid N_2 employing the BET method. The phases present in the catalysts were determined by the X-ray diffraction (XRD) using the Rigaku D/Max-RA diffractometer with a Cu Kα radiation source (λ = 0.15418 nm). The applied voltage and current were 40 kV and 50 mA, respectively. TPR was performed by using a quartz U-tube reactor loaded with about 50 mg of a sample. A mixture of N_2 and H_2 (5.13% H_2 by volume) was used and the flow rate was maintained at 40 ml/min. The hydrogen consumption was monitored using a thermal conductivity detector (TCD). The reducing gas was first passed through the reference arm of the TCD before entering the reactor. The reactor exit was directed through a trap filled with $Mg(ClO_4)_2$ (to remove water) and then to the second arm of the TCD. The temperature was raised at a programmed rate of 10 K/min from 303 to 1173 K.

Microcalorimetric adsorption of NH_3 was carried out on a Tian-Calvet heat-flux apparatus. The microcalorimeter was connected to a gas handling and volumetric adsorption system, equipped with a Baratron capacitance manometer (MKS, USA) for precision pressure measurement. The differential heat of adsorption versus adsorbate coverage was obtained by measuring the heats evolved when doses of a gas (2–5 μmol) were admitted sequentially onto the catalyst until the surface was saturated by the adsorbate. Ammonia with a purity of 99.99% was used. Before microcalorimetric measurements, the samples were typically dried under vacuum, calcined in 67 kPa O_2, and evacuated, respectively, at 673 K for 1 h. The microcalorimetric adsorption was performed at 423 K.

The Fourier transform infrared spectroscopy (FTIR) measurements for NH_3 adsorbed samples were recorded with a Bruker Vector 22 FTIR spectrograph. The samples were self-sustaining wafers with 13 mm in diameter and a thickness of about 20 mg/cm^2. A wafer was usually treated in 67 kPa O_2 at 673 K for 1 h, followed by evacuation for 2 h. About 1.33–2.66 kPa NH_3 was introduced and then evacuated at room temperature for 30 min. The IR spectra of the surface species were obtained by subtracting the blank from the spectra with adsorbed ammonia.

2.3. Catalytic reactions

The probe reaction was carried out in a fixed-bed glass tube reactor (ϕ12). About 100 mg of a sample was loaded for the reaction. Isopropanol was introduced to the reaction zone by bubbling air (60 ml/min) through a glass saturator filled with isopropanol maintained at 295 K. Isopropanol and reaction products were analyzed by an on-line gas chromatograph, using a PEG 20M packed column connected to an FID. Each catalyst was pretreated by heating in air at 673 K for 1 h and then cooled in air flow to the reaction temperature.

The reaction of selective oxidation of toluene was performed by using a U-tube fixed-bed microreactor (ϕ12) loaded with a sample of about 0.5 g with 20–40 meshes. The reactants were fed into the reactor by bubbling air through a glass saturator filled with toluene maintained at 330 K. In each test, the reaction reached steady state after 1 h on stream before the tail gas was analyzed by using an on-line gas chromatograph. The organic compounds were separated by an FFAP capillary column and detected by an FID while CO_x was detected by using a Hayesep D packed column and a TCD.

3. Results and discussion

3.1. Structure characterization

Fig. 1 shows the XRD patterns for the V-Zr-O catalysts with different V_2O_5 contents. V_2O_5 and ZrO_2 prepared in this work are typically orthorhombic (JCPDS 09-0387) and cubic (JCPDS

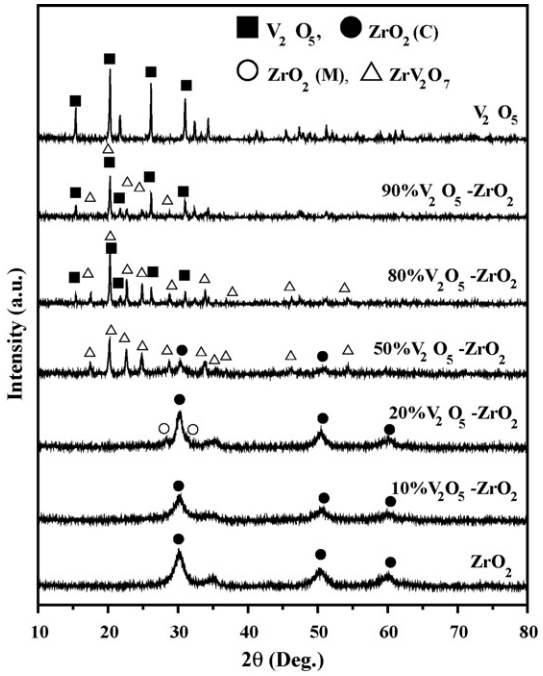

Fig. 1. X-ray diffraction patterns of ZrO_2, V_2O_5 and the V-Zr-O catalysts.

Table 1
Surface areas of ZrO_2, V_2O_5 and the V-Zr-O complex oxides

V_2O_5 (wt.%)	0	10	20	50	80	90	100
Surface area (m^2/g)	59	71	35	10	10	7	6

27-0997), respectively. The 10% V_2O_5-ZrO_2 catalyst exhibited only cubic ZrO_2 without any other phases, implying the well-dispersed vanadium species on the surface of ZrO_2. The 20% V_2O_5-ZrO_2 catalyst also exhibited mainly cubic ZrO_2, but with a small amount of monoclinic ZrO_2 (JCPDS 83-0944). However, ZrV_2O_7 (JCPDS 16-422) became the main phase in the 50% V_2O_5-ZrO_2. In fact, ZrO_2 was disappeared in the complex oxides when the content of V_2O_5 was higher than 80%, and the main phases detected in these samples were ZrV_2O_7 and V_2O_5. It should be mentioned that, since the strongest diffraction peak of V_2O_5 and ZrV_2O_7 overlapped around 20°, the two phases were identified according to their other characteristic peaks.

Table 1 presents the surface areas of the V-Zr-O catalysts with various V_2O_5 contents. The surface area of ZrO_2 and V_2O_5 was 59 and 6 m^2/g, respectively. The surface area of the 10% V_2O_5-ZrO_2 was 71 m^2/g, higher than that of ZrO_2. The surface areas were decreased for the complex oxides with V_2O_5 more than 20%, which might be due to the formation of new phase ZrV_2O_7 in the samples.

3.2. Surface acidic and redox properties

Fig. 2 shows the TPR profiles of the catalysts. There were two weak TPR peaks around 882 and 960 K for ZrO_2, which could be due to the reduction of Zr^{4+} to Zr^{3+} on the surface and subsurface [26,27]. Four TPR peaks occurred at 931, 959, 1018 and 1125 K for V_2O_5, corresponding to the sequential reductions: $V_2O_5 \rightarrow V_6O_{13} \rightarrow V_2O_4 \rightarrow V_6O_{11} \rightarrow V_2O_3$ [28]. The broad TPR peak at 806 K for the 10% V_2O_5-ZrO_2 and that at 813 K for the 20% V_2O_5-ZrO_2 might be assigned to the reduction of vanadium species highly dispersed in the lattice of ZrO_2. The reduction temperature (806–813 K) of such vanadium species was much lower than those of bulk V_2O_5 (931–1125 K), implying the promotion effect of ZrO_2 on the reduction of vanadium species. One main TPR peak at 881 K was observed for the 50% V_2O_5-ZrO_2, which could be attributed to the reduction of ZrV_2O_7 since XRD revealed that the sample possessed mainly ZrV_2O_7 with some ZrO_2. The sample 80% V_2O_5-ZrO_2 contained ZrV_2O_7 and V_2O_5 and the temperatures for the reduction of this sample increased significantly. There were five TPR peaks for the 90% V_2O_5-ZrO_2 sample. This TPR profile appeared as if a superimposition of those for the V_2O_5 and 80% V_2O_5-ZrO_2.

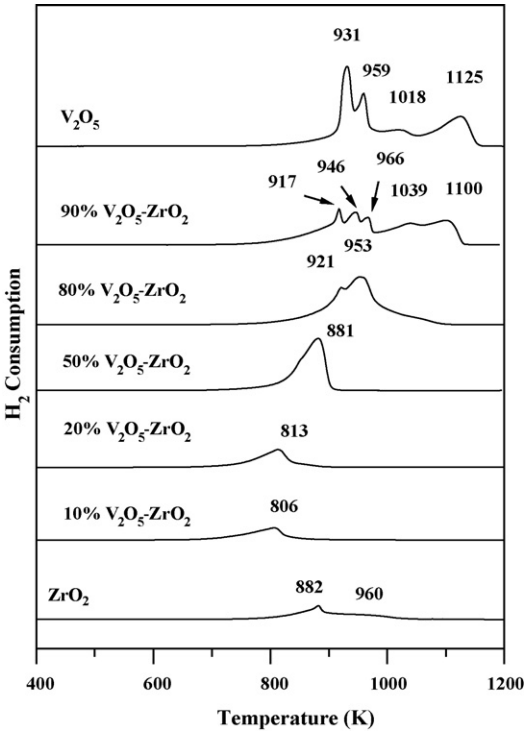

Fig. 2. TPR profiles of ZrO_2, V_2O_5 and the V-Zr-O catalysts.

The areas of the reduction peaks of the V-Zr-O samples were calculated quantitatively. Suppose that the area of the total reduction peaks for V_2O_5 is 100, the areas of the samples with V_2O_5 content of 90, 80, 50, 20, 10 and 0% were, thus, calculated to be 90, 78, 47, 20, 17 and 20, respectively. It seemed that above 20% V_2O_5 content, the areas of the reduction peaks were proportional to the V_2O_5 contents in V-Zr-O oxides, suggesting that only vanadia species in the complex oxides were reduced. Zirconia species began to reduce when V_2O_5 content was lower than 10%. These results are in agreement with those reported in the literatures [26–28], which stated that bulk V_2O_5 could be completely reduced to V_2O_3 and only surface and subsurface Zr^{4+} of bulk ZrO_2 were reduced to Zr^{3+}, when the reduction temperature was up to 1200 K.

The results of microcalorimetric adsorption of NH_3 for the samples are shown in Fig. 3. The ZrO_2 exhibited quite strong surface acidity with the initial heat of 228 kJ/mol and the saturation coverage of 340 μmol/g, respectively. On the other hand, the V_2O_5 prepared in this work showed the low surface acidity with the initial heat of 59 kJ/mol and the saturation coverage of 128 μmol/g for the adsorption of ammonia. The incorporation of 10% V_2O_5 did not seem to have a significant effect on the surface acidity of ZrO_2. The addition of 20% V_2O_5 decreased the initial heat to 198 kJ/mol and the saturation coverage to 235 μmol/g,

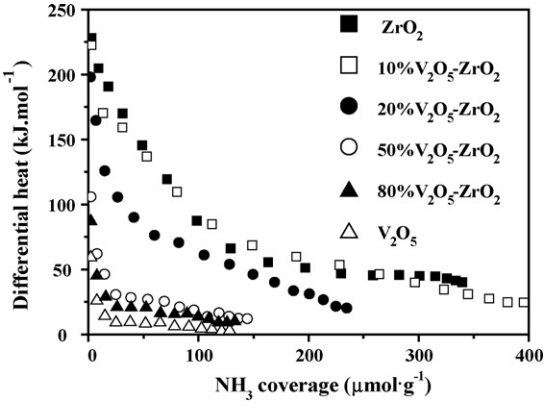

Fig. 3. Differential heats versus coverage for NH_3 adsorption at 423 K on the V_2O_5, ZrO_2 and V-Zr-O catalysts.

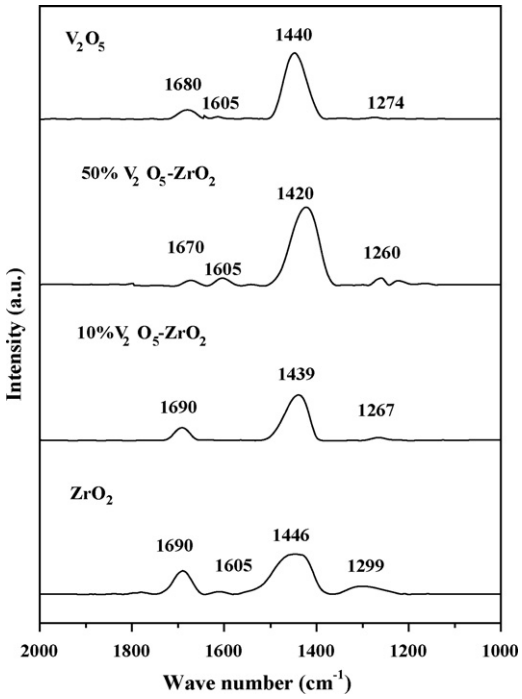

Fig. 4. FTIR spectra for NH_3 adsorption at room temperature on ZrO_2, V_2O_5 and the V-Zr-O catalysts.

indicating the significantly decreased surface acidity. The surface acidity was further decreased when more V_2O_5 was added. In fact, the complex oxides with V_2O_5 more than 50% exhibited the weak surface acidity as that of V_2O_5, since the initial heat and saturation coverage for the adsorption of ammonia were similar for these samples. The formation of ZrV_2O_7 seemed the reason for the weakened surface acidity.

Fig. 4 shows the FTIR spectra for ammonia adsorption on ZrO_2, V_2O_5 and the typical V-Zr-O complex oxides. It is generally believed that the IR peaks around 1393, 1450 and 1680 cm^{-1} are due to the vibrations of NH_4^+ produced by the NH_3 adsorption on Brønsted acid sites, while the peaks around 1610 and 1230–1260 cm^{-1} are due to the coordinatively adsorbed NH_3 on Lewis acid sites [29,30]. Thus, all the samples displayed mainly the Brønsted acidity with the IR peaks around 1440 and 1680 cm^{-1} as well as a small amount of Lewis acidity with the IR peaks around 1270 and 1605 cm^{-1} for the adsorbed ammonia.

The isopropanol probe reaction has been extensively used to characterize the surface acid/base properties. It is generally true that isopropanol converts to propylene and diisopropyl ether on acid sites while converts to acetone on base sites when the reaction is performed in an inert atmosphere. However, when the reaction is carried out with the presence of O_2, isopropanol can be oxidized to acetone, which may be used to characterize the redox property of a catalyst [31–34].

Fig. 5 presents the results for the probe reaction of isopropanol on ZrO_2, V_2O_5 and V-Zr-O catalysts in air at 453 K. The conversion of isopropanol was close to 100% on ZrO_2 with 100% selectivity to propylene. This result indicated that the ZrO_2 used in this work was highly acidic without any redox ability for the oxidative dehydrogenation of isopropanol. The addition

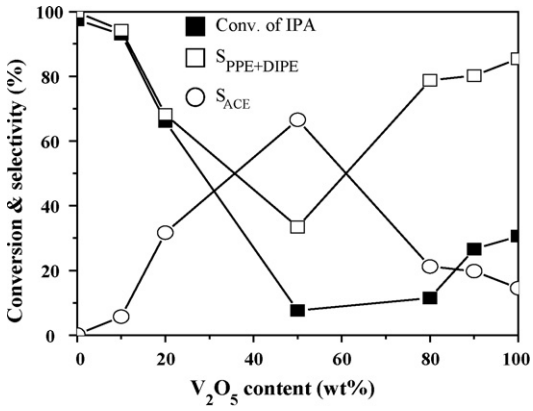

Fig. 5. Conversion of isopropanol (IPA) and selectivity to propylene (PPE), diisopropyl ether (DIPE) and acetone (ACE) on ZrO_2, V_2O_5 and the V-Zr-O complex oxides in air at 453 K.

of V_2O_5 up to 50% significantly decreased the conversion of isopropanol as well as the selectivity to propylene. Meanwhile, the selectivity to acetone was increased up to 67%. These results clearly indicated the decreased surface acidity and the increased redox ability of the samples upon the addition of V_2O_5. The bulk V_2O_5 exhibited mainly the surface acidity with some redox ability since it produced much more propylene than acetone for the conversion of isopropanol in air. The 50% V_2O_5-ZrO_2 exhibited the low conversion of isopropanol (8%) with 27% selectivity to propylene and 67% selectivity to acetone, respectively, indicating the weak surface acidity and relatively stronger redox ability of the sample. These results demonstrated such a fact that the combination of two acidic oxides might produce a complex oxide (e.g., ZrV_2O_7) with significantly decreased surface acidity and enhanced redox ability. Thus, it is possible to monitor the surface acidic and redox properties of a series of complex oxides by varying their compositions to meet the needs of catalysis.

3.3. Selective oxidation of toluene

Table 2 gives the results for the selective oxidation of toluene over ZrO_2, V_2O_5 and V-Zr-O with different compositions. The products were found to be benzaldehyde, benzoic acid and CO_2. ZrO_2 is not active since it lacks redox ability. The complex oxides containing 10–50% V_2O_5 exhibited fairly well activities for the selective oxidation of toluene. The conversion of

Table 2
Selective oxidation of toluene over ZrO_2, V_2O_5 and the V-Zr-O catalysts at 633 K

V_2O_5 (%)	Conversion (%)	Selectivity (%)			Yield (%)
		Benzaldehyde	Benzoic acid	Total	Total
0	0.4	33	0	33	0.1
10	20	39	14	53	11
20	24	33	24	57	14
50	21	35	28	63	13
80	18	33	4	37	7
90	15	30	8	38	6
100	9	22	16	38	3

toluene was similar (about 20%) on these catalysts though their surface areas were quite different. The conversion of toluene on V_2O_5 was low (9%). The addition of 10% ZrO_2 increased the conversion of toluene to 15%. Thus, the complex oxides V_2O_5-ZrO_2 seemed more active than V_2O_5, which might be due to the presence of V-O-Zr bonds in V_2O_5-ZrO_2. The total selectivity to benzaldehyde and benzoic acid over the 80% V_2O_5-ZrO_2, 90% V_2O_5-ZrO_2 and V_2O_5 was similar (37–38%), reflecting mainly the property of V_2O_5, agreeing with the XRD and TPR results. The total selectivity to benzaldehyde and benzoic acid over the 10% V_2O_5-ZrO_2, 20% V_2O_5-ZrO_2 and 50% V_2O_5-ZrO_2 was relatively higher (53–63%).

The catalysts could be classified into three categories according to their catalytic behavior for the selective oxidation of toluene. ZrO_2 itself forms a category. It possesses acidity only and lacks the redox ability and, therefore, it is not active for the selective oxidation of toluene. The second category includes the 80% V_2O_5-ZrO_2, 90% V_2O_5-ZrO_2 and V_2O_5, which exhibited the catalytic behavior similar to V_2O_5. The 10% V_2O_5-ZrO_2, 20% V_2O_5-ZrO_2 and 50% V_2O_5-ZrO_2 may be grouped into the third category. These catalysts displayed the similar catalytic behavior for the selective oxidation of toluene, typical of the V_2O_5-ZrO_2 complex oxides. It should be mentioned that the catalysts in the third category exhibited the similar TPR profiles with only one reduction peak for each sample and the peak temperatures were much lower than those of V_2O_5. The lower reduction temperatures implied the stronger redox abilities and, therefore, the higher activity for the selective oxidation of toluene. In addition, XRD results indicated the presence of ZrV_2O_7 in the 20% V_2O_5-ZrO_2 and it became the main phase in the 50% V_2O_5-ZrO_2. Although no ZrV_2O_7 was observed in the 10% V_2O_5-ZrO_2 by XRD, the presence of highly dispersed ZrV_2O_7 on the surface of 10% V_2O_5-ZrO_2 could not be excluded. Suppose that the surfaces of the three catalysts in the third category were covered by ZrV_2O_7, it would not be strange that the three catalysts displayed the similar catalytic behavior. It seems that the formation of ZrV_2O_7 or the V-O-Zr bonds in the complex oxide catalysts benefits the selective oxidation of toluene for the production of benzaldehyde and benzoic acid. Since ZrO_2 was the main phase in the 10% V_2O_5-ZrO_2 with possibly some highly dispersed ZrV_2O_7, it is quite natural that the sample behaved like the bulk ZrO_2 in some aspects. For example, it exhibited quite strong surface acidity like ZrO_2 as revealed by the microcalorimetric adsorption of ammonia and the isopropanol probe reaction. This is probably the reason why this sample exhibited lower selectivity as compared with other two catalysts in the third category. It should be mentioned that the TPR profile of the 10% V_2O_5-ZrO_2 is completely different from that of ZrO_2. The peak temperature of 10% V_2O_5-ZrO_2 was significantly decreased as compared to that of ZrO_2. Considering the facts that the 10% V_2O_5-ZrO_2 showed relatively high activity while ZrO_2 was almost not active for the selective oxidation of toluene, the TPR peak of 10% V_2O_5-ZrO_2 must mainly be the result of the reduction of vanadium species in the sample, not the reduction of Zr^{4+}. Such TPR and catalytic results can be taken as the indirect evidence for the existence of surface ZrV_2O_7 in the 10% V_2O_5-ZrO_2. It should be emphasized that with the increase of ZrV_2O_7, the complex oxide catalysts in the third category exhibited significantly lower surface acidity, relatively stronger redox ability and higher selectivity for the formation of benzaldehyde and benzoic acid. The complex oxides 80% V_2O_5-ZrO_2 and 90% V_2O_5-ZrO_2 might contain V_2O_5 that covered the ZrV_2O_7, leading to the catalytic behavior similar to that of bulk V_2O_5.

4. Conclusion

V-Zr-O complex oxide catalysts with wide compositions were prepared by the sol–gel method. XRD revealed that ZrV_2O_7 was the main phase in the 50% V_2O_5-ZrO_2. This catalyst exhibited high selectivity to acetone for the conversion of isopropanol in air, revealing its weak surface acidity and relatively stronger redox ability, agreeing with the results of microcalorimetric adsorption of ammonia and TPR. The complex oxides with low content of V_2O_5 showed the strong surface acidity and produced mainly propylene for the conversion of isopropanol in air. The strong surface acidity decreased the selectivity to benzaldehyde and benzoic acid for the oxidation of toluene. On the other hand, V_2O_5 might cover the surface of the complex oxides with high content of V_2O_5, leading to the lowered selectivity to benzaldehyde and benzoic acid. The formation of ZrV_2O_7 or V-O-Zr bonds seemed to benefit the selective oxidation of toluene. In addition, TPR results clearly showed that the V_2O_5-ZrO_2 complex oxides were significantly easier reduced than the single oxides, indicating the stronger redox ability of the complex oxides. The results from the microcalorimetric adsorption of ammonia and the isopropanol probe reaction in air further revealed the decreased surface acidity and enhanced redox ability of the complex oxides. Therefore, the formation of suitable V-O-M bonds to decrease the surface acidity and meanwhile to enhance the redox ability seemed to be a way to improve the catalytic behavior for the selective oxidation of toluene.

Acknowledgements

Financial supports from NSFC (20233040 and 20673055), MSTC (2005CB221403) and Jiangsu Province, China (BG2006031) are acknowledged.

References

[1] A. Sabatini, G. Sloli, CA Patent 817,920 (1969), to Snia Viscosa.
[2] A. Antoni, R. Vincenzo, CA Patent 773,590 (1967), to Snia Viscosa.
[3] P.P. Rossi, M. Catoni, US Patent 4,349,473 (1980), to Snia Viscosa.
[4] http://www.qrx.cn/.
[5] X. Ge, H.L. Zhang, J. Fan, Chin. J. Catal. 19 (1998) 42–46.
[6] W.X. Kuang, Y.N. Fan, K.D. Chen, Y. Chen, J. Catal. 186 (1999) 310–317.
[7] G. Centi, S. Perathoner, S. Tonini, Catal. Today 61 (2000) 211–221.
[8] D.A. Bulushev, L. Kiwi-Minsker, V.I. Zaikovskii, O.B. Lapina, A.A. Ivanov, S.I. Reshetnikov, A. Renken, Appl. Catal. A 202 (2000) 243–250.
[9] S. Larrondo, A. Barbaro, B. Irigoyen, N. Amadeo, Catal. Today 24 (2001) 179–187.
[10] F. Konietzni, H.W. Zanthoff, W.F. Maier, J. Catal. 188 (1999) 154–164.
[11] H.L. Zhang, W. Zhong, X. Duan, X.C. Fu, J. Catal. 129 (1991) 426–437.

[12] H.L. Zhang, W. Zhong, X. Ge, X.C. Fu, CN Patent 92,107,558.8 (1992), to Nanjing Univ.
[13] A. Brückner, Appl. Catal. A 200 (2000) 287–297.
[14] N. Shimizu, N. Saito, M. Ueshima, Stud. Sur. Sci. Catal. 44 (1988) 131–138.
[15] D.A. Bulushev, L. Kiwi-Minsker, V.I. Zaikovskii, A. Renken, J. Catal. 193 (2000) 145–153.
[16] A. Bottino, G. Capannelli, A. Comite, R.D. Felice, Catal. Today 99 (2005) 171–177.
[17] M. Ponzi1, C. Duschatzky, A. Carrascull, E. Ponzi, Appl. Catal. A 169 (1998) 373–379.
[18] F. Konietzni, U. Kolb, U. Dingerdissen, W.F. Maier, J. Catal. 176 (1998) 527–535.
[19] M.H. Zahedi-Niaki, S.M.J. Zaidi, S. Kaliaguine, Appl. Catal. A 196 (2000) 9–24.
[20] S.C. Su, A.T. Bell, J. Phys. Chem. B 102 (1998) 7000–7007.
[21] J.R. Sohn, S.G. Cho, Y.I. Pae, S. Hayashi, J. Catal. 159 (1996) 170–177.
[22] A. Christodoulakis, M. Machli, A.A. Lemonidou, S. Boghosian, J. Catal. 222 (2004) 293–306.
[23] J.R. Sohn, I.J. Doh, Y.I. Pae, Langmuir 18 (2002) 6280–6288.
[24] X.T. Gao, J.M. Jehng, I.E. Wachs, J. Catal. 209 (2002) 43–50.
[25] C.L. Pieck, M.A. Bañares, J.L.G. Fierro, J. Catal. 224 (2004) 1–7.
[26] T.M. Yu, R.X. Zhou, Z.M. Tang, X.M. Zheng, Chem. J. Chin. U. 20 (1999) 123–126.
[27] A.L. Borer, C. Brönnimann, R. Prins, J. Catal. 145 (1994) 516–525.
[28] H. Bose, B.J. Kip, J.G.V. Ommen, P.J. Gellings, J. Chem. Soc. Faraday Trans. I 80 (1984) 2479–2488.
[29] J. Shen, R.D. Cortright, Y. Chen, J.A. Dumesic, J. Phys. Chem. 98 (1994) 8067–8073.
[30] H. Knözinger, Adv. Catal. 25 (1976) 184–271.
[31] A. Gervasini, J. Fenyvesi, A. Auroux, Catal. Lett. 43 (1997) 219–228.
[32] D. Haffad, A. Chambellan, J.C. Lavalley, J. Mol. Catal. A 168 (2001) 153–164.
[33] D. Kulkarni, I.E. Wachs, Appl. Catal. A 237 (2002) 121–137.
[34] X.D. Gu, J.Z. Ge, H.L. Zhang, A. Auroux, J.Y. Shen, Thermochim. Acta 451 (2006) 84–93.